Supporting Information

Defects and self-trapped excitons regulation in rare-earth doped all-inorganic perovskite

Anshi Chu,‡[a] Jun Luo,‡[a] Zheyuan Xu,[b] Yunfei Xie,[b] Wenjie Luo,[b] Siyao Li,[a] Jieyuan Liang,[a] Junyu He,[a] Chi Zhang,[a] Mengqiu Cai,[a] Xiujuan Zhuang*[c]

a. School of Physics and Electronics, Hunan University, Changsha 410082, China. Email: mqcai@hnu.edu.cn

b. College of Materials Science and Engineering, School of Physics and Electronic Science, Hunan University, Changsha 410082, China

c. College of Semiconductors (College of Integrated Circuits), Hunan University, Changsha 410082, China. Email: zhuangxj@hnu.edu.cn

‡ These authors contributed equally to this work.

* Corresponding authors (Email: zhuangxj@hnu.edu.cn)

The supporting information includes Figures S1-S13

Supporting Information Catalog

1, Materials Growth

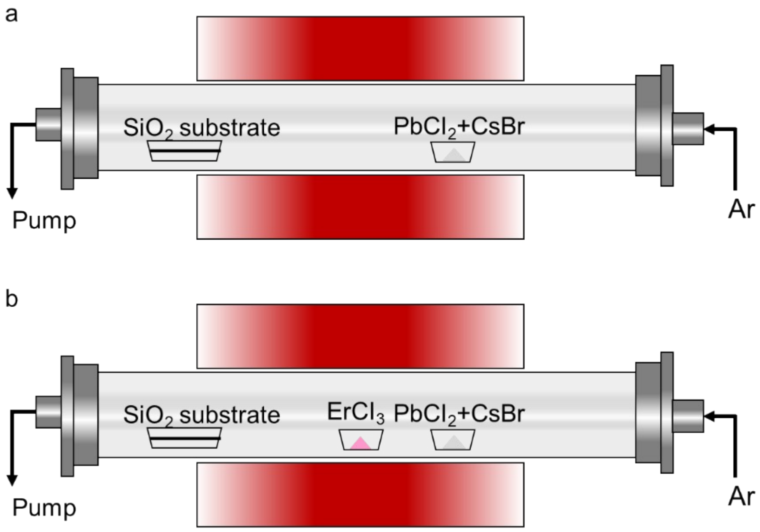

Figure S1. Schema of chemical vapor deposition setup of (a) undoped- and (b) Er-doped $CsPbCl_{3x}Br_{3(1-x)}$.

Table S1. Temperatures distribution in the quartz tube.

Distance to Furnace Tube Center (cm)	Temperature (°C)	Distance to Furnace Tube Center (cm)	Temperature (°C)
0	832	9	740
1	832	9.5	707
2	830	10	671
3	828	10.5	621
4	824	11	570
5	818	11.5	510
6	811	12	448
7	798	12.5	388
8	779		

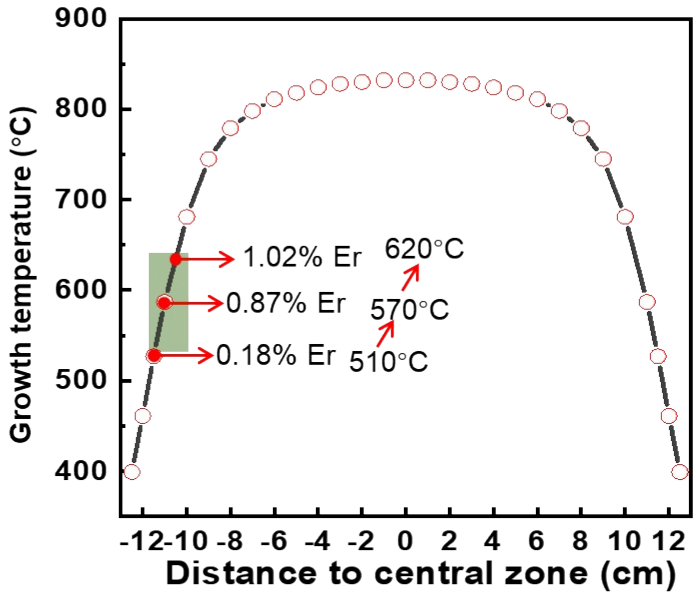

Figure S2. Temperature control and distribution corresponding to Er-doping samples. The optimized temperatures used to grow S1 (0.18% Er-doping), S2 (0.87% Er-doping), and S3 (1.02% Er-doping) are 520, 570, and 620 °C, respectively.

2, Materials Characterizations

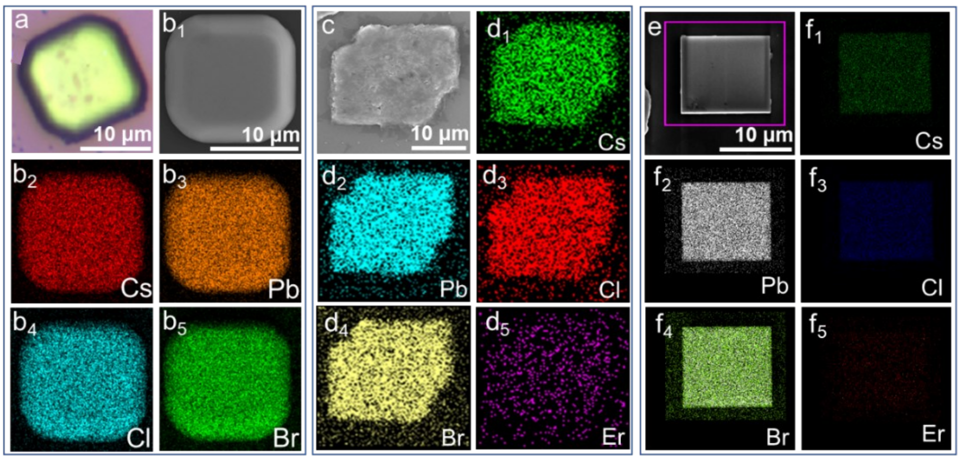

Figure S3. Characterization of undoped- and Er-doped $CsPbCl_{3x}Br_{3(1-x)}$. (a) optical image and (b) SEM image of undoped $CsPbCl_{3x}Br_{3(1-x)}$. (b_1-b_5) Elemental mappings of Cs, Pb, Cl, and Br in the MP shown in panel b. (c) SEM image of 0.87% Er-doped $CsPbCl_{3x}Br_{3(1-x)}$. (d_1-d_5) Elemental mappings of Cs, Pb, Cl, Br, and Er in the MP shown in panel c. (e) SEM image of 1.02% Er-doped $CsPbCl_{3x}Br_{3(1-x)}$. (f_1-f_5) Elemental mappings in the MP shown in panel e.

Table S2. The molar percentage of Er, Cs, Pb, Cl, and Br in pure $CsPbCl_{3x}Br_{3(1-x)}$ and Er-doped $CsPbCl_{3x}Br_{3(1-x)}$ grown at 510, 570, 620 °C.

Weight (%)	Growth temperature (°C)	Er	Cs	Pb	Cl	Br	Cs+Pb	Cl+Br
Atomic fraction	510	0.18	20.07	19.88	33.60	26.26	39.95	59.86
		0.46	21.04	20.89	36.03	21.58	41.93	57.61
	570	-	19.73	19.91	24.22	36.14	39.64	60.36
		0.81	19.98	21.62	37.53	20.06	41.60	57.59
		0.87	23.23	15.95	20.89	39.06	39.18	59.06
	620	1.02	22.89	19.57	25.17	31.34	42.46	56.51
		1.46	21.40	21.59	31.08	24.47	42.99	55.55

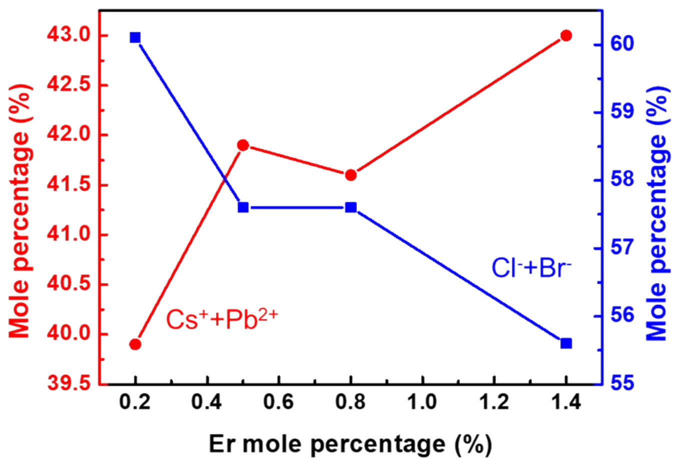

Figure S4. The molar percentage of (Cs^{+}+Pb^{2+}) and (Cl^{-}+Br^{-}) as a function of the molar percentage of Er^{3+}.

Table S3. The molar percentage of Cs, Pb, Cl, and Br in pure $CsPbCl_{3x}Br_{3(1-x)}$ grown at 510, 570, 620 °C.

Weight (%)	Growth temperature (°C)	Er	Cs	Pb	Cl	Br	Cs+Pb	Cl+Br
Atomic fraction	510	20.4	20.1	31.6	27.9	40.5	59.5	20.4
		19.5	19.9	31.5	29.1	39.4	60.6	19.5
	570	20.0	19.7	31.1	29.2	39.7	60.3	20.0
		20.0	20.2	31.6	28.2	40.2	59.8	20.0
	620	19.7	19.9	28.7	31.7	39.6	60.4	19.7
		20.3	20.1	28.6	31.0	40.4	59.6	20.3
	Average mole					40.0	60.0	

ratio

3, Optical characterization of undoped and Er-doped $CsPbBr_{3x}Cl_{3(1-x)}$.

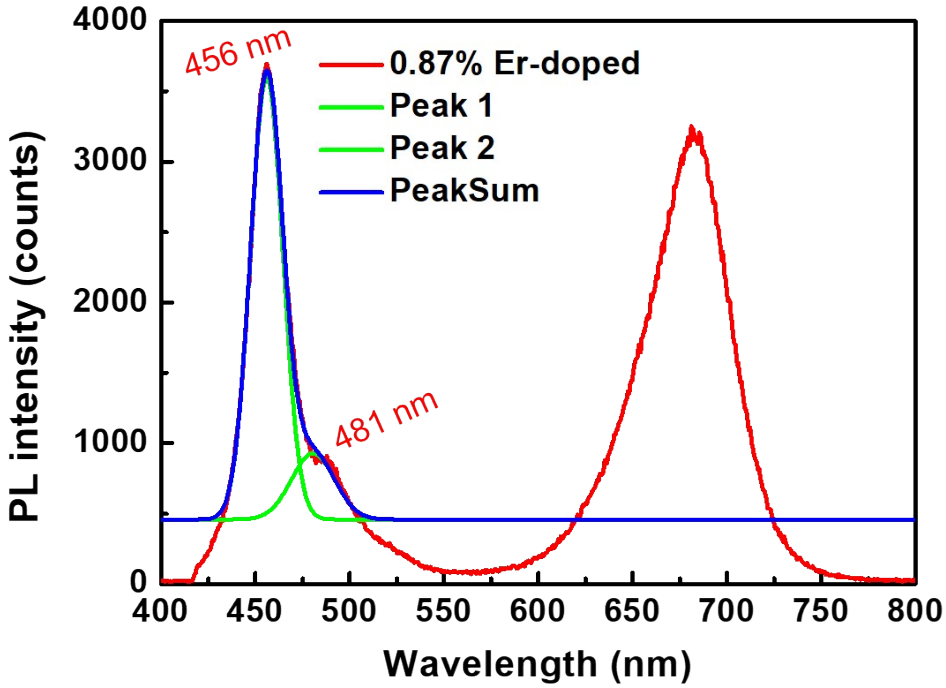

Figure S5. PL spectrum and bimodal Gaussian fitting of band-edge emission at 456 nm of 0.87% Er-doped $CsPbBr_{3x}Cl_{3(1-x)}$.

Table S4. The molar percentage of Er, Cl, Br in pure, 0.87% Er, and 1.02% Er-doped $CsPbCl_{3x}Br_{3(1-x)}$ with emission peaks at 481nm, 481 (456)nm, and 475 nm.

Sample	Er (%)	Cl (%)	Br (%)	Cl/Br	Cl/(Cl+Br)
Pure (481nm)	0	24.2	36.2	0.67	0.4
0.87%-Er (481nm (456nm))	0.9	20.9	39.1	0.53	0.35
0.87%-Er (475nm)	1.0	25.2	31.3	0.81	0.45

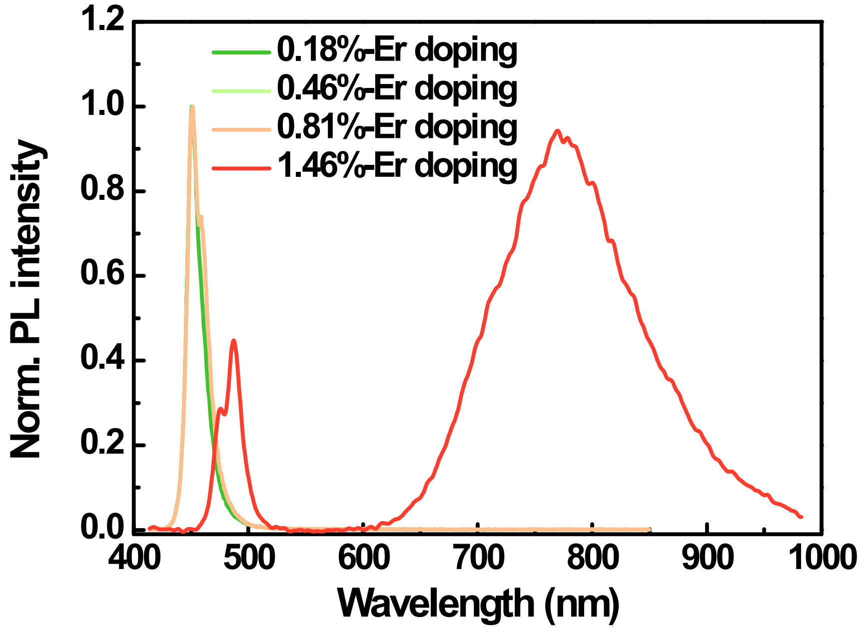

Figure S6. PL spectra of 0.18%, 0.46%, 0.81%, and 1.46% Er-doped $CsPbBr_{3x}Cl_{3(1-x)}$.

4, Dynamics analysis for the undoped- and Er-doped $CsPbCl_{3x}Br_{3(1-x)}$.

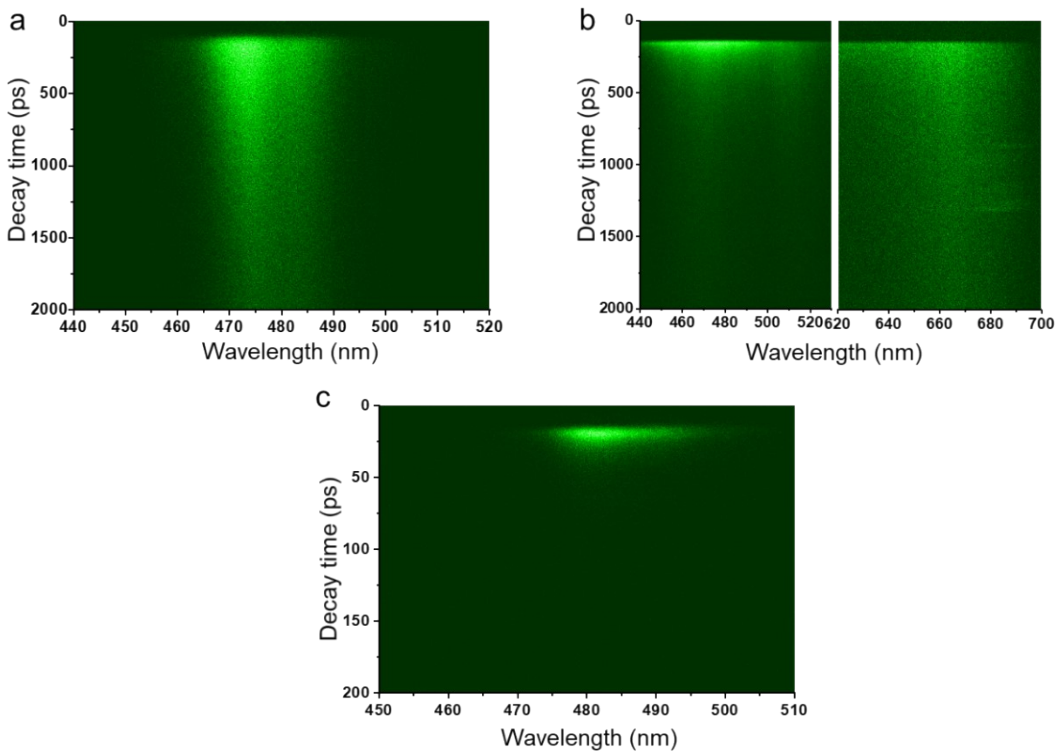

Figure S7. Streak camera images of (a) undoped, (b) 0.87%, and (c) 1.02% Er-doped $CsPbCl_{3x}Br_{3(1-x)}$.

Table S5. Fitting parameters of the dynamic curves for narrowband emission of the undoped, 0.87%, and 1.02% Er-doped $CsPbCl_{3x}Br_{3(1-x)}$.

	τ_1 (ps)	A_1(%)	τ_2 (ps)	A_2(%)	$\tau_{average}$ (ps)
481nm	504.7	77.4	2474.4	22.6	1664
456 nm	92.3	78.0	596.1	22.0	417.5
475 nm	5.2 ps	75.5	13.0 ps	24.5	8.7

The decay curves are fitted by a biexponential function: $I(t) = A_1 e^{-t/\tau_1} + A_2 e^{-t/\tau_2}$,[1] and the average PL lifetime is calculated by the formula: $\tau_{average} = \frac{a_1\tau_1^2 + a_2\tau_2^2}{a_1\tau_1 + a_2\tau_2}$.

Table S6. Fitting parameters of the dynamic curves for broadband emission of the 0.87% and 1.02% Er-doped $CsPbCl_{3x}Br_{3(1-x)}$.

	τ_1 (ps)	A_1(%)	τ_2 (ps)	A_2(%)	$\tau_{average}$ (ps)
683 nm	269.6	56.9	1874.8	43.1	1868.7
810 nm	2.3 ns	7.4	0.7 ns	92.6	1.03 ns

The decay curves are fitted by a biexponential function: $I(t) = A_1 e^{-t/\tau_1} + A_2 e^{-t/\tau_2}$, and the average PL lifetime is calculated by the formula: $\tau_{average} = \frac{a_1\tau_1^2 + a_2\tau_2^2}{a_1\tau_1 + a_2\tau_2}$.

5, Power-dependent PL spectra for 1.02% Er-doped $CsPbCl_{3x}Br_{3(1-x)}$.

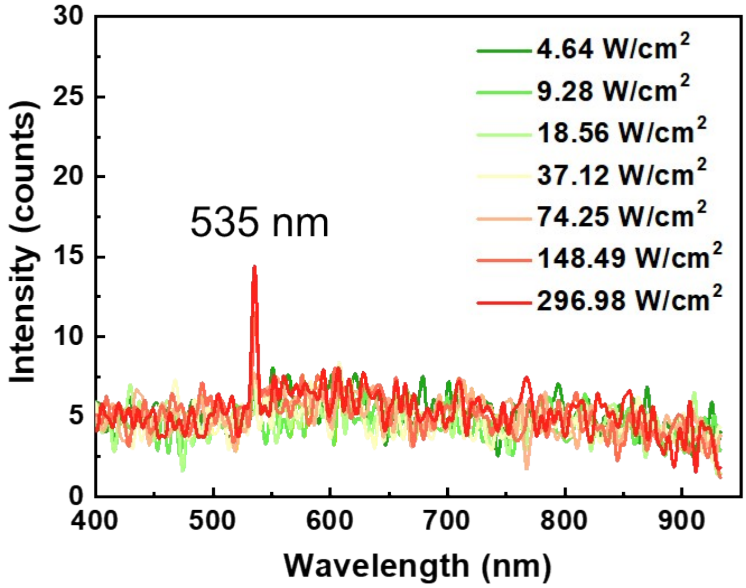

Figure S8. Excitation power-dependent PL spectra of the 1.02% Er-doped $CsPbBr_{3x}Cl_{3(1-x)}$ for an excitation wavelength of 532 nm. Excitation power: 4.64-296.98 W/cm^2). A continuous laser with a wavelength of 532nm was used to excite 1.02%-Er-doped $CsPbCl_{3x}Br_{3(1-x)}$, and the 1.02%-Er dopped sample cannot be excited. When the excitation power is higher than 74.25 W/cm^2, the peak at 535nm is the remaining laser after the 532nm long-pass filter.

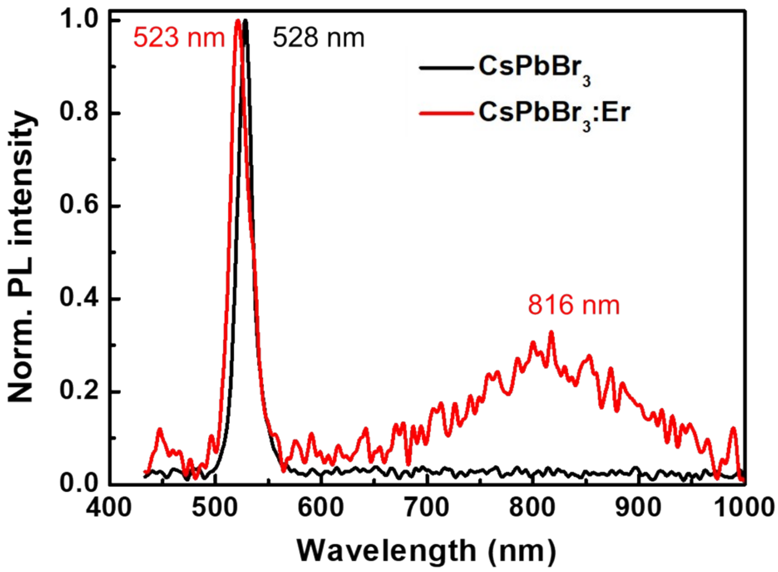

Figure S9. PL spectra of $CsPbBr_3$ and Er-doped $CsPbBr_3$.

6, Computational Methods

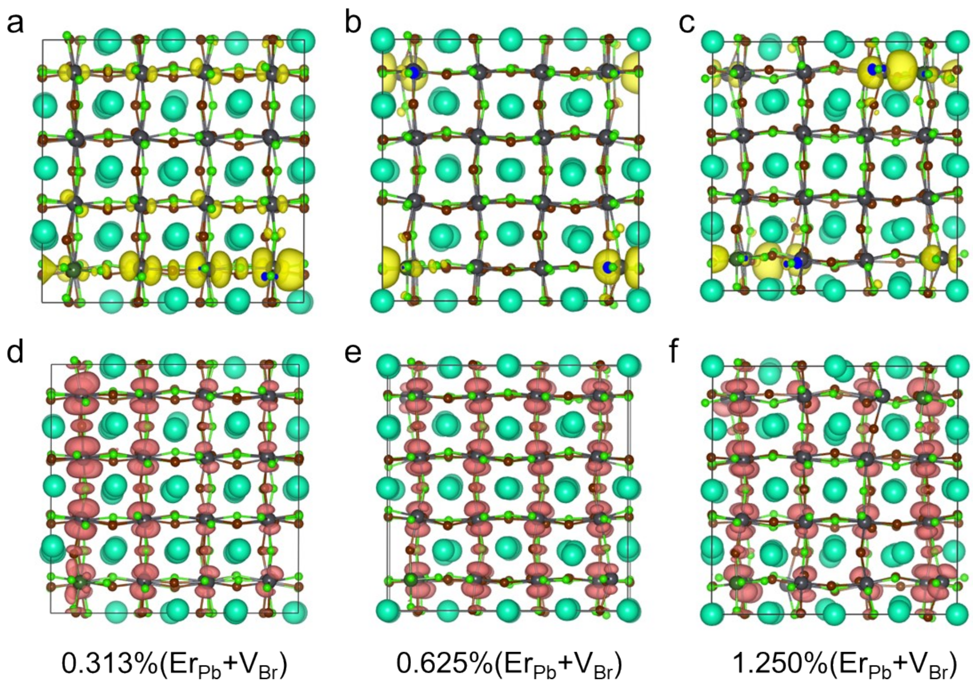

Figure S10. The partial charge densities of holes and of electrons $CsPbCl_{3x}Br_{3(1\text{-}x)}$ under different doping concentrations. (a-c) is the density of holes electrons, and (d-f) is the density of electrons.

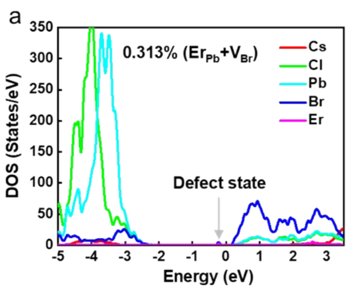

Figure S11. The projected density of states of material $CsPbCl_{3x}Br_{3(1\text{-}x)}$ under different Er doping concentrations. (a-c) represent the projected density of states when the doping concentrations are 0.313%, 0.625%, and 1.250%, respectively.

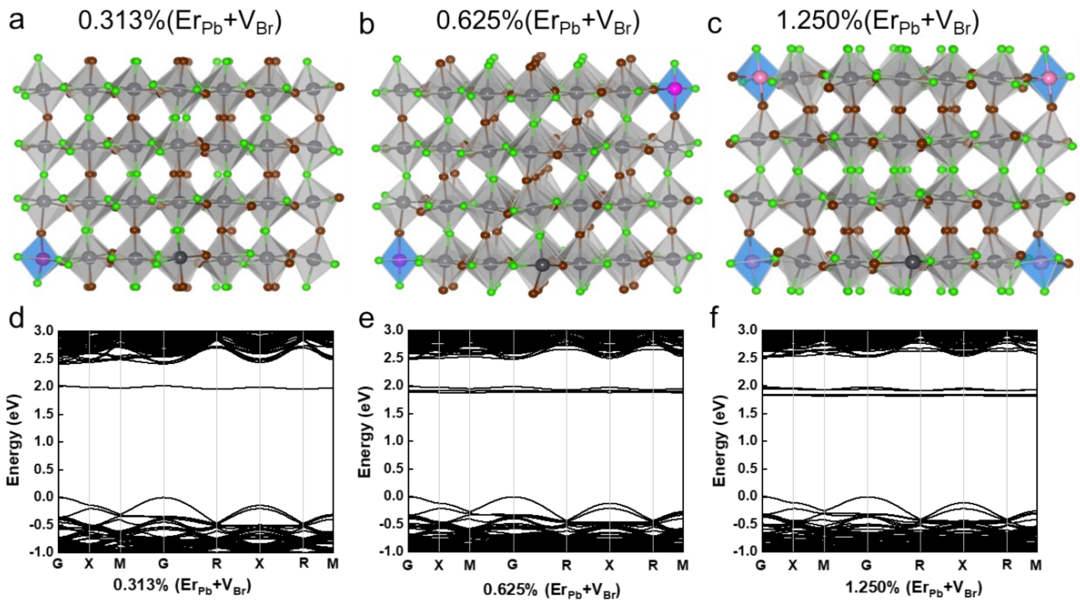

Figure S12. (a-c) is the optimized crystal structures, and (d-f) is band structure of $CsPbCl_{3x}Br_{3(1\text{-}x)}$ doped with 0.313%, 0.625%, and 1.250% Er ions with Br vacancies.